ORIGINAL ARTICLE
(CC BY-SA)
UDC: 616.9-084:615.479.4
DOI: https://doi.org/10.2298/VSP230922025J

Antivirus and antibacterial filters for face masks based on silver quantum dots

Antivirusni i antibakterijski filteri za maske za lice na bazi srebrnih kvantnih tačaka

Vukoman Jokanović*†, Nemanja Zdravković‡, Božana Petrović*, Marija Živković§, Vladimir Biočanin‖, Ema Aleksić‖, Jovana Milutinović‖, Tamaš Petrović¶

University of Belgrade, *National Institute of the Republic of Serbia, Institute of Nuclear Sciences "Vinča", §Faculty of Dental Medicine, Clinic of Orthodontics, Belgrade, Serbia; †ALBOS doo, Belgrade, Serbia; ‡Scientific Veterinary Institute of Serbia, Belgrade, Serbia; ‖University Business Academy in Novi Sad, Faculty of Stomatology in Pančevo, Pančevo, Serbia; ¶Scientific Veterinary Institute "Novi Sad", Novi Sad, Serbia

Abstract

Background/Aim. Available face masks, used to protect the respiratory system from various types of pathogens, show unsatisfactory efficiency because the size of viruses like severe acute respiratory syndrome coronavirus 2 (SARS-CoV-2) is much smaller than the void spaces in these masks. Difficult breathing through some masks quickly tires out, which makes ordinary people avoid wearing them. These facts suggest that a new strategy is desirable for designing protective face masks. The aim of the study was to present new filters for face masks to protect people exposed to high concentrations of bacteria and viruses, particularly SARS-CoV-2. **Methods.** Filters for these masks were manufactured of dense cotton fabric impregnated with silver quantum dots. The filters were characterized by scanning electron microscopy and ion-coupled plasma mass spectrometry. Wettability properties were determined by measuring contact angles with water, and a color fastness test was performed. Antibacterial assay was performed using *Staphylococcus (S.) aureus*. Viability quantitative polymerase chain reaction (qPCR) for virus integrity assay and reverse transcription qPCR (RT-qPCR) assay were used for antiviral activity assessment. **Results.** *In vitro* assays showed extremely high efficiency of these filters in destroying *S. aureus* and SARS-CoV-2 virus. The filters also showed high safety and easy breathing possibilities. **Conclusion.** The high efficiency of these masks against SARS-CoV-2 has been demonstrated through numerous tests, and they have been approved as anti-SARS-CoV-2 masks for the first time in the world. In the meantime, this solution has been applied in practice, and the data obtained about that are very encouraging.

Key words:
air filters; masks; polymerase chain reaction; sars-cov-2; silver; staphylococcus aureus.

Apstrakt

Uvod/Cilj. Dostupne maske za lice, koje se koriste za zaštitu respiratornog sistema od različitih vrsta patogena, ne pokazuju zadovoljavajuću efikasnost, jer je virus poput korona virusa izazivača teškog akutnog respiratornog sindroma, *severe acute respiratory syndrome coronavirus 2* (SARS-CoV-2) mnogo manji od pora u ovim maskama. Teško disanje kroz neke maske brzo dovodi do zamora, zbog čega ljudi izbegavaju da ih nose. Te činjenice sugerišu da je poželjna nova strategija u dizajniranju zaštitnih maski za lice. Cilj rada bio je da se predstave novi filteri za maske za zaštitu osoba izloženih visokoj koncentraciji bakterija i virusa, posebno SARS-CoV-2. **Metode.** Filteri za te maske izrađeni su od guste pamučne tkanine impregnirane srebrnim kvantnim tačkama. Filteri su okarakterisani skenirajućom elektronskom mikroskopijom i jonsko-spregnutom plazma masenom spektrometrijom. Svojstva vlaženja određivana su merenjem kontaktnih uglova sa vodom, a ispitana je i postojanost boje tih filtera. Antibakterijski test izveden je korišćenjem *Staphylococcus* (*S.*) *aureus*. Za procenu antivirusne aktivnosti korišćeni su test viabilnosti *quantitative polymerase chain reaction* (qPCR) – test integriteta virusa i test reverzne transkriptaze qPCR (RT-qPCR). **Rezultati.** *In vitro* testovi pokazali su izuzetno visoku

Correspondence to: Vukoman Jokanović, ALBOS d.o.o., Orahovačka 19, 11 000 Belgrade, Serbia. E-mail: vjokan@gmail.com

efikasnost ispitanih filtera u uništavanju bakterije *S. aureus* i virusa SARS-CoV-2. Filteri su, takođe, pokazali visoku sigurnost i mogućnost za lako disanje. **Zaključak.** Visoka efikasnost ispitivanih maski protiv SARS-CoV-2 dokazana je mnogobrojnim testovima i one su, po prvi put u svetu, odobrene kao anti-SARS-CoV-2 maske. U međuvremenu, ovo rešenje primenjeno je u praksi, a podaci o tome su veoma ohrabrujući.

Ključne reči:
filteri; maske, hirurške; polimeraza, reakcija stvaranja lanaca; sars-cov-2; srebro; staphylococcus aureus.

Introduction

For the last three years, we have witnessed a pandemic of severe acute respiratory syndrome coronavirus 2 (SARS-CoV-2), which has taken many lives. As a primary preventive measure, the mandatory wearing of face masks has been required in many countries. The World Health Organization (WHO) has recommended filtering facepiece (FFP) masks as a protection standard [1, 2]. However, they have shown low efficiency in highly virulent environments and difficult breathing. FFP2 masks guarantee the retention of objects larger than 2.5 μm, and when it comes to significantly smaller viruses than porous channels, like SARS-CoV-2, they cannot provide sufficient protection. With FFP3 masks, breathing is tough, but even that way, they do not protect against the virus effectively because the size of the virus is 2–3 times smaller than the diameter of the channels in these masks. All these facts and frequent mutations of SARS-CoV-2 and the weak effect of existing vaccines on each subsequent mutation require an entirely new approach to designing face masks to protect against viruses such as SARS-CoV-2. Shortness of breath with FPP masks makes them extremely unpopular, which is why more and more people refuse to use the mask at all [3–6].

Our concept is based on manufacturing textile filters for face masks with pronounced super-hydrophobic, physical, and biological self-cleaning properties against bacteria and viruses. For textiles with a fibrous structure on a micro-scale, this strategy assumes the application of nanoscale silver particles to the fiber surface to achieve a micro/nanoscale structure necessary to achieve the minimum textile surface energy requirement [7, 8]. The methods most commonly used for preparing robust super-hydrophobic textile surfaces include physical and chemical approaches, coating, wet chemical deposition, electro-assisted chemical deposition, spray application, sol-gel process, chemical etching, chemical deposition, and plasma treatment *in situ* by nanotube/particle growth, chemical vapor deposition and plasma processing technique [9, 10].

The filter's surface super-hydrophobicity, influenced by an appropriate hierarchical structure that enables a very high wetting angle of water droplets (above 150°), prevents the penetration of aerosols with SARS-CoV-2 inside of filter [11]. Physical self-cleaning mainly mimics the surface of a lotus leaf and is characterized by the water contact angle and the angle of sliding. Biological self-cleaning properties assume an active reaction of the filters impregnated with silver quantum dots with SARS-CoV-2 and bacteria and their efficient destruction [2, 12].

As it is well known, viral infectivity is the capability of a virus to enter the host cell and use its resources to reproduce [13]. The interaction of the virus with the host cell occurs thanks to the protein capsid, which contains antigens specific to cell receptors that provide virus entrance into the cell. In addition, the capsid has a protective function for the viral genome from degradation by nucleases and physical influences. Damage to the viral capsid decreases or annuls its capacity to protect the viral genome and its ability to replicate in the host, meaning that the intact viral capsid is crucial for a successful infection. If the relationship between damage to the viral capsid and degradation of the viral genome is established, the detection of the viral genome can be correlated with the infectivity of the virus [14]. This method enables measuring the efficiency of filters impregnated with silver quantum dots in bacterial and virus (SARS-CoV-2) destruction, which is applied in this study.

The aim of this study was to present a new approach we applied to produce face masks based on the manufacturing of superhydrophobic, antibacterial, and anti-corona virus disease (COVID) active filters as the middle layer of a three-layer mask. These filters showed extremely high efficiency in destroying *Staphylococcus* (*S.*) *aureus* bacteria and SARS-CoV-2 virus in *in vitro* investigations.

Methods

Manufacturing of textile filters

Filters for face masks are manufactured of dense cotton fabric impregnated with silver (Ag) quantum dots and named ALBO nanosilver filters (Fs). *In situ*, the formation of Ag nanoparticles on swollen cellulose fibers of dense cotton fabric implies the immersion of cellulose fibers in potassium hydroxide (KOH), which enables uniform distribution of Ag ions (Ag^+) within the cellulose matrix in the subsequent phases of the (Cell-COOK)-cellulose with activated carboxyl (COOH) group by potassium ions, transforming it into COOK activated form. In addition, alkali pretreatment raised pH to ≈12, which plays an important role in reducing Ag^+ to Ag^0. When Ag nitrate ($AgNO_3$) is added to the cellulose in an alkaline solution, Ag^+ diffuses well within the swollen cellulose, and intense interaction of Ag^+ and/or complexes between Ag^+ and cellulose functional groups (COO-K and OH groups) occurs. By increasing the temperature to 70 °C, using borohydride as a reducing reagent, the reduction of Ag^+ to nano size of Ag^0 within the cellulose matrix is intensified [2, 15]. Through such a procedure, the reduction process is further catalyzed. The obtained composite structure is additionally stabilized by the sterile effect of

cellulose chains. Finally, un-impregnated Ag nanoparticles are removed from the dyed fibers by rinsing under a strong water jet [16]. The described method was modified in a specific experiment of obtaining ALBO nanosilver Fs to accelerate the reduction process to the maximum and create as many nucleation centers of nanosilver quantum dot clusters as possible. The procedure details are described in the patent application, and only the most important structural and functional properties of ALBO nanosilver Fs are presented in this paper.

Scanning electron microscopy and energy dispersive X-ray spectroscopy analysis

The morphology of the cotton fabric before and after Ag impregnation was determined by scanning electron microscopy (SEM), equipped with energy dispersive X-ray spectroscopy-EDS (FESEM-EDS, FEI SCIOS 2, Dual-beam).

Inductively coupled plasma spectroscopy

Ion-coupled plasma mass spectrometry quantification was performed using the instrument Thermo Scientific iCAP 6500 Duo ICP (Thermo Fisher Scientific, Cambridge, United Kingdom) with iTEVA operating software.

Wetting angle

Wetting angles were estimated with a goniometer equipped with a unique optical system and a charge-coupled device (CCD) camera. A drop of liquid (5 μL) was placed on a specially prepared plate of the substrate, and the image was immediately sent *via* the CCD camera to the computer for analysis. For contact angle estimation, the L-M and L-Q methods were used.

Color fastness

Briefly, since the ALBO nanosilver Fs were painted, it was easy to identify their color change after washing. These tests were performed in a 50:1 liquid ratio in a 2 L of water mixed with 5.0 g/L of standard soap solution inside a closed 2 L rotating container constant (washing fastness tester GT-D07) at a speed and 40 °C and 60 °C during 30 min. Evaluation of color fastness after 5, 10, and 15 washing cycles was performed on a grayscale according to ISO-05-A02 (loss of color depth) and ISO-105-AO3 (degree of color), and the same was cross-checked by measuring color loss and color loss using Macbeth 2020 plus measurement system color associated with the appropriate software. The resistance of the paint to rubbing (dry and wet) was assessed according to ISO: 766-1984 method using a grayscale according to ISO-105-AO3 (staining range), after which the tested samples were graded according to the change of color intensity and their coloring on gray. The grayscale is used to identify the score in half steps 5, 4–5, 4, 3–4, 3, 2–3, 2, 1–2, and 1 using the SDCE Grey Scale device. The scale in half of the steps consists of pairing gray patterns, from 5 – good (un-washed cotton fabric sample impregnated with nanosilver) to 1 – bad (white, un-impregnated sample). Each pairing illustrates the difference in hue between the tested and control samples, which corresponds to the numbered score.

Antibacterial assay

This assay was derived by using the horizontal method for the enumeration of microorganisms through colony count at 30 °C, with the surface plating technique, following the ISO 6888-1:1999/Amd 1:2,003. The obtained results were given in the original reference of the certified laboratory for food and drugs of the Veterinary Institute in Belgrade, Serbia. Briefly, nano-Ag-impregnated fabric was tested against *S. aureus* ATCC 25923. The inoculum was formed by the standard procedure for antimicrobial susceptibility testing ISO 20776-1. Overnight cultures of *S. aureus* were suspended in physiologic saline (NaCl 0.9%) solution in distilled water at pH 6.5 with a concentration of McFarland 0.5 1–2 10^8 [colony forming unit (CFU)/mL] and further serial diluted in eight decimal steps using sterile saline. The vials of bacterial suspensions were then incubated with agitation at 220 revolutions *per* min (rpm) for 2 hrs, at 37 ± 2 °C, which enabled the preparation of a homogenous suspension of bacteria. The tested cotton fabric samples, with dimensions 50 × 60 mm, were sterilized before testing by an autoclave device in moisturized heat (121 °C) for 15–20 min in Petri dishes (90 mm glass dish). Sterile cotton fabric specimens were then placed in sterile Petri dishes and inoculated with 2 mL of inoculums. After 4 hrs of incubation at room temperature, materials were impressed on the agar surface, and residue inoculum fluids were placed on agar (ISO 7218) to determine the remaining viable bacteria count.

Antiviral assay for SARS-CoV-2

Experimental setup: SARS-CoV-2 virus isolate SARS-CoV-2/human/SRB/NSNIVNS01 (NCBI GenBank MW485928) of 4th blind passage, isolated in the Scientific Veterinary Institute Novi Sad, Serbia in April 2020 was used for experimental setup. The virus was isolated on the VERO cell line (ATCC CCL-81) by standard virus isolation technique. The virus cytopathic effect appeared in the first blind passage on VERO cells. The titer of the virus used in the experiment on VERO cell culture was $10^{5.0}$ $TCID_{/50}$ in 0.1 mL. Firstly, the Ag-impregnated fabric was moistened with distilled water; then, it was appropriately squeezed (centrifuged at 15,000 rpm for 15 min and supernatant excluded) and cut into squares with dimensions 1.5 × 1.5 cm. Then, six such squares were placed in microtubes of 2 mL volume and soaked with 100 μL of SARS-CoV-2 virus isolate (in duplicate). These squares of Ag-impregnated fabric were exposed to the virus in the microtubes for 60 min. After the specified time, 900 μL of tissue culture medium, without fetal calf serum, was added to each sample; tested squares were squeezed several times with micropipette

tips onto the microtube sides and vigorously shaken on the vortex. The same procedure was done with the fabrics without Ag as a negative control in duplicate samples. For RNA extraction, 200 μL of each tested sample was used (three virus samples treated with Ag-impregnated fabric, in duplicate; two virus samples treated with the fabric without Ag as negative controls, in duplicate; SARS-CoV-2 virus isolate used for the experiment as virus control, in triplicate). Half the prepared samples were first put on ice and later used for RNA extraction. The other half of the samples were first treated with propidium monoazide (PMA)xx dye [viability polymerase chain reaction (PCR)]. The RNA extraction and subsequently real-time reverse transcription (RT) PCR [real-time RT-PCR or RT-quantitative PCR (qPCR)] for all the samples were done at the same time as described below. All samples subjected to real-time RT-PCR detection of SARS-CoV-2 were tested in duplicate.

Viability qPCR – virus integrity assay

Since molecular methods cannot distinguish infectious and noninfectious particles, the infectivity of SARS-CoV-2 samples both before and after the contact/incubation on/with Ag-impregnated fabric was predicted by treating the samples with the nucleic acid intercalating dye PMAxx (50 μmol/L) and Triton 100-X surfactant (0.5%), followed by photoactivation, which catalyzes stable cross-linking between PMAxx and any nucleic acid molecules to which it has access, before RT-qPCR. This enabled the distinction between virions with unchanged and modified capsids [17–20]. The difference (reduction) in RT-qPCR signal between the treated and control aliquot – Δ cycle threshold (C_t) (ΔC_t), which refers to the difference in RT-qPCR C_t, correlates with the portion of the target RNA in the sample which is associated with inactivated virions [21]. Viability assays were carried out by treating 200 μL of SARS-CoV-2 viral load samples exposed/incubated with Ag-impregnated fabric, then SARS-CoV-2 viral load samples exposed/incubated with the ordinary fabric without Ag and unexposed virus control samples with 50 μM PMAxx (Biotium) and 0.5% Triton 100-X (Thermo Fisher Scientific, Roma, Italy) in DNA LoBind 1.5 mL tubes (Eppendorf, Germany) in the dark at room temperature for 15 min in a shaker at 400 pm. Following an incubation period, to obtain a covalent bond with PMAxx and RNA, the viral suspensions were immediately exposed to 15 min photoactivation using a photoactivation system (PMA-Lite™ LED Photolysis Device, Biotinum, CA, US). After photo-induced cross-linking with light emitted by blue light-emitting diodes (LEDs), samples were processed for RNA extraction and the PMAxx untreated paired samples and subsequently subjected to RT-qPCR amplification.

Nucleic acid extraction and molecular analysis

SARS-CoV-2-specific RNA was detected using an RT-qPCR assay. Following instructions by manufacturers, RNA was extracted from virus isolates supernatants after the treatment of the Ag-impregnated cotton fabric, non-impregnated cotton fabric, and virus-positive and negative controls by using the KingFisher Flex System (Thermo Fisher, Waltham, MA, USA) and extraction kit BioExtract SuperBall (Biosellal, France). Detection of SARS-CoV-2 RNA was performed using the detection of the part of the RNA-dependent RNA polymerase gene (RdRp) in an RT-PCR protocol (Charité, Berlin) according to the WHO guidelines [22]. Primer sets used are forward RdRP_SARSr-F2 (5'-GTGARATGGTCATGTGTGGCGG-3') and reverse RdRP_SARSr-R1 (5'-CARATGTTAAASACACTATTAGCATA-3') with the probe RdRP_SARSr-P2 5'-FAM-CAGGTGGAACCTCATCAGGAGATGC-BBQ-3'. The RT-qPCR was carried out using the SuperScript III Platinum One-Step RT-qPCR Kit (ThermoFisher, USA) on an ABI PRISM 7500 Fast Real-Time PCR System (Applied Biosystems, USA). The positive control for real-time RT-qPCR was isolated SARS-CoV-2/human/SRB/NSNIVNS01 (NCBI GenBank MW485928). Nuclease-free water was used as the negative control, while a Ct treshold of 40 was regarded as cut-off to consider the test negative [22]. RT-qPCR Extraction Control Red (MDX028, Meridian Bioscience, UK) was used according to the manufacturer's recommendation as RNA extraction and RT-qPCR internal control of reaction.

S. aureus was used in this assay as an ever-evolving, well-known pathogen with a complicated set of virulence factors, which lures from human and animal surroundings and even food [23–27]. On the other hand, Ag is known for its antibacterial effect in different states [28–32].

Molecular techniques using qPCR are robust, cost-efficient, highly sensitive, and specific; they have the severe limitation of not being able to differentiate between infectious and noninfectious virus particles [33, 34]. One of the most established qPCR modifications to measure infectivity is capsid integrity qPCR, an approach where samples are pre-treated with the intercalating azo dyes PMA, ethidium monoazide (EMA) or their derivate PMAxx and photo-reactive azide forms of phenanthridium - PEMAX [18–20, 35–38]. The technique is based on the principle that an azo dye, applied to the examined sample before the virus genome extraction procedure, can only enter virions with a damaged capsid to covalently and irreversibly bind with viral DNA or RNA after activation with light emitted by high-energy lamps or blue LEDs. This pretreatment can block the amplification of nucleic acids due to the detachment of the polymerase when it encounters the dye-genome complex [35]. Subsequently, only genomic targets that originate from intact virions are amplified, while those genome nucleic acids that were outside the virions (that belong to noninfectious viruses) at the time of the nucleic acid extraction procedure will not be amplified during the qPCR.

Results

The structure and distribution of cotton fibers (CFs) in dense cotton fabric used in ALBO nanosilver Fs are clearly visible in the SEM image (Figure 1). The fibers' thickness is

about 15 μm, and they are intertwined throughout the cotton fabric in bundles wide about 300 μm.

After impregnation, small dots of quantum size Ag are clearly visible on CFs (Figure 2). The EDS analysis showed that these fibers contain Ag quantum dots of about 1.1 mass %, while the quantities of C and O are 31.9 and 63.9 mass %.

The release of the Ag^+ or small clusters of Ag from bonded Ag quantum dots is very low, decreasing significantly with increasing time of immersion of ALBO nanosilver Fs in hot water (60 °C) (Table 1). The release rates are 4.47 ppb/h for the first 4 hrs, 1.37 ppb for the next 8 hrs, 0.89 ppb for the next 12 hrs, and finally 0.24 ppb for the next 48 hrs. These values are almost negligible, even for the first 4 hrs.

The contact angle between water droplets and ALBO nanosilver Fs was measured (Figure 3, Table 2). These data indicate a strong hydrophobicity of the filter surface.

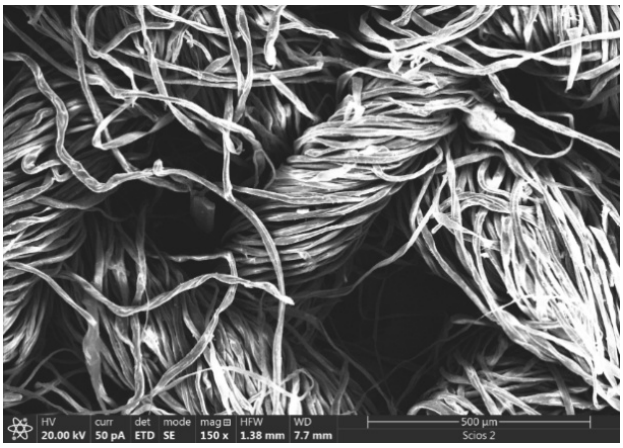

Fig. 1 – Scanning electron microscopy: typical appearance of fibers in cotton fabric before silver impregnation (magnification × 150).

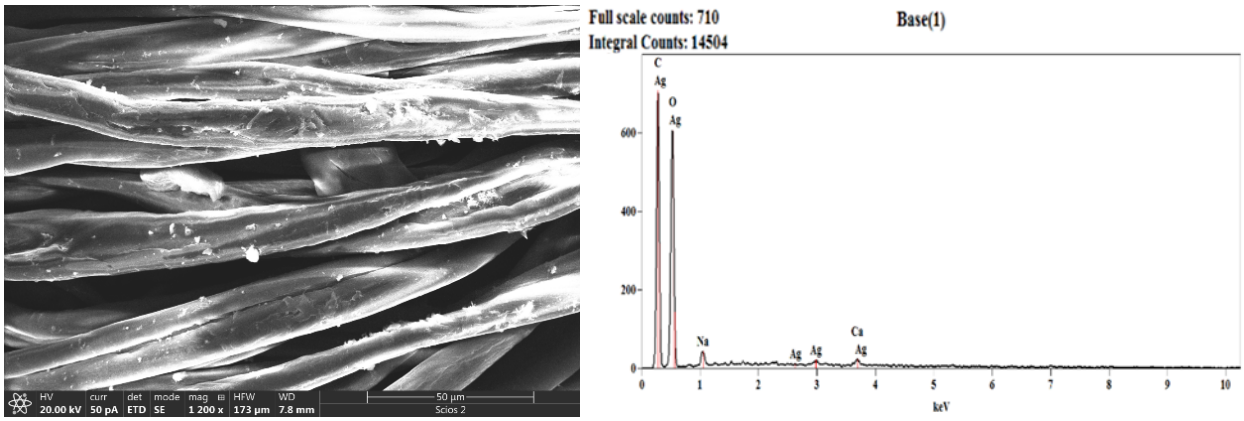

a) **b)**

Fig. 2 – a) Scanning electron microscopy: A typical appearance of silver (Ag) impregnated cotton fabric fibers (magnification × 1,200); b) energy dispersive X-ray spectroscopy.

Table 1

Released concentrations of silver (Ag) during the various immersion times in hot water at 60°C

Immersion time (hrs)	Concentration of Ag (ppb)
1	21.7 ± 0.2
4	39.5 ± 0.2
12	50.5 ± 0.5
24	61.2 ± 1.0
72	72.97 ± 0.9

hrs – hours; ppb – part per billion.

Results are presented as mean ± standard deviation.

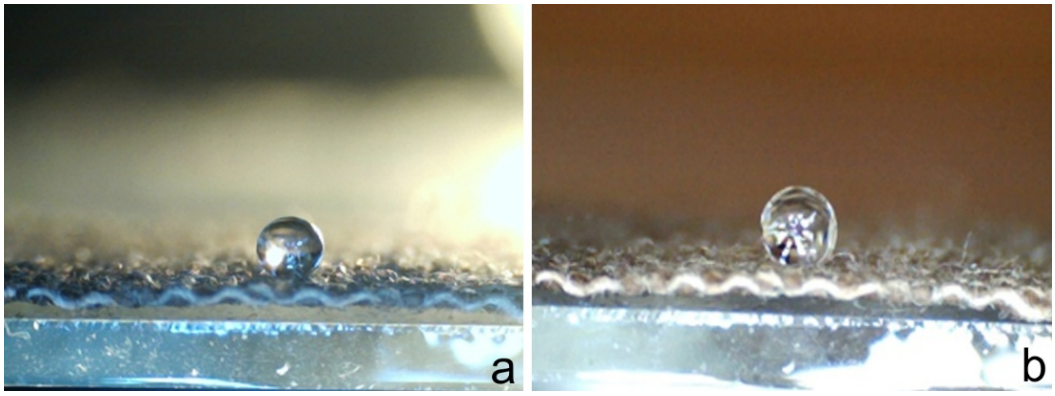

Fig. 3 – The typical appearance of the micro-droplet at the surface of ALBO nanosilver filter. Magnification x 400 (a), x 600 (b).

Table 2

Contact angle between the water droplet and the surface of ALBO nanosilver filters

Filter parameters	Values
Contact angle, °	144
	141
	131
	139
	143
Average value, °	139.6
Error, °	14

In all washing cases, the color fastness of the Ag-impregnated cotton fabric during rubbing in wet conditions was lower than in dry conditions. Final treatment with poly-carboxyl acid probably improves bonding strength, especially in wet conditions, between Ag quantum dots and CFs, as shown in Table 3.

From the obtained results, even in inoculums over 10^5 CFU/mL, a slight reduction of inoculums can be observed, while on 10^4 CFU/mL, this reduction was evident. When ALBO nanosilver Fs is used in contact with the initial load of inoculated bacteria order of 1.5×10^3 CFU/mL, this number decreased to 320 CFU/mL, while in non-impregnated material, this number reduced to 1,691 CFU/mL (CFU counts after 1.5×10^3 CFU/mL is presented in Figure 4). This indicated that ALBO nanosilver Fs induces a huge reduction of viable bacteria absorbed on its surfaces (Figures 4–6).

Described setup of tested samples (both PMAxx untreated and treated tested nanosilver quantum dots-impregnated fabric samples, fabrics without nanosilver quantum dots as negative control samples for nanosilver quantum dots; SARS-CoV-2 virus as virus positive controls; water samples as virus negative controls) were presented in Tables 4 and 5.

This difference translated to the number of viral particles detectable between the genome of SARS-CoV-2 exposed to the test materials – ALBO nanosilver Fs and untreated virus control samples, i.e., reduction of the viral load of the genome, ranged from 1.03 to 1.23 $\log_{10}$, with an average value of 1.14 $\log_{10}$ of detectable viral genome particles.

Table 3

Shade and fastness properties of ALBO nanosilver filters

Parameters	Values
Wash times	0
	5
	10
	15
Wet color change	5
	4–5
	4–5
	3–4
Wet color staining	–
	5
	4
	4

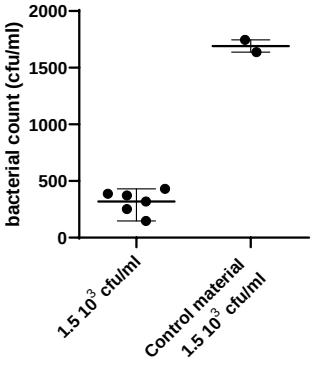

Fig. 4 – Reduction in colony forming unit (CFU) counts on nanosilver-impregnated and non-impregnated cotton fabric after 4 hrs of incubation under the load of 1.5×10^3 CFU/mL.

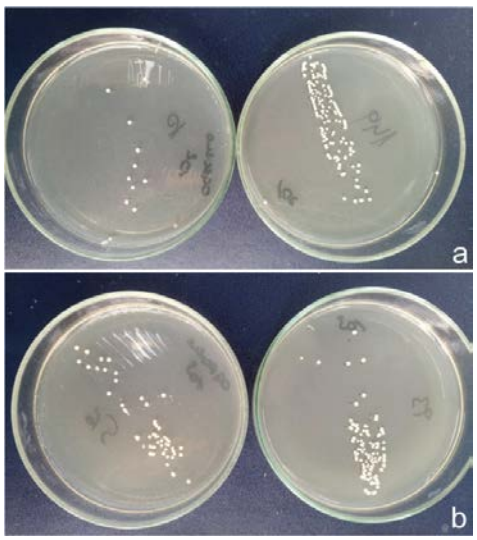

Fig. 5 – Bacterial counts on nanosilver-impregnated material (left) and non-impregnated cotton fabric (right) under the load of a) 10^2 colony-forming units (CFU)/mL and b) 10^3 CFU/mL.

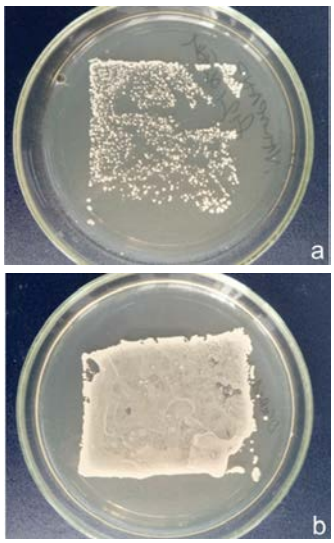

Fig. 6 – Nanosilver impregnated material impress on a) agar surface and b) control cotton fabric after 4 hrs on incubation under 1–2 × 10^8 colony forming units/mL.

Table 4

Results of influence of ALBO nanosilver quantum dots filter on SARS-CoV-2 virus loads and viability with PMAxx

Label of sample	Test samples		Internal control[#]
	Labels	Ct values SARS-CoV-2	Ct values
ALBO nanosilver quantum dots filter, incubation with virus 60 min	1	19.52	38.59
	1	19.33	38.51
	2	19.18	38.41
	2	19.24	36.22
	3	19.46	38.44
	3	19.34	34.84
	1P	37.65	32.44
	1P	37.67	32.32
	2P	38.59	32.04
	2P	38.63	31.95
	3P	38.50	32.03
	3P	39.00	32.02
Filter without nanosilver quantum dots layers, incubation with virus 60 min	K1	18.79	36.38
	K1	18.90	34.98
	K2	18.60	36.76
	K2	18.55	36.25
	K1 P	35.43	31.81
	K1 P	35.30	31.50
	K2 P	35.16	32.39
	K2 P	35.93	31.72

SARS-CoV-2 – severe acute respiratory syndrome coronavirus 2; PMA – propidium monoazide.

1, 2, and 3 – samples of virus treated nanosilver quantum dots impregnated fabric in duplicate; K1 and K2 – samples of virus treated ordinary fabric without nanosilver quantum dots as nanosilver negative controls in duplicate; 1P, 2P, and 3P – the same as samples 1, 2, and 3 just treated with PMAxx dye for 15 min (viability assay); K1P and K2P – the same as samples K1 and K2 just treated with PMAxx dye for 15 min (viability assay); PC – virus positive control – unexposed virus control sample (SARS-CoV-2 virus isolate used for the experiment) in triplicate; PC-P – the same as PC just treated with PMAxx dye for 15 min (viability assay); water sample as negative control of the experiment in triplicate; NTC – non template control – polymerase chain reaction (PCR) reagents control on virus contaminaton in triplicates; [#] – internal control used in extraction and RT-qPCR as control of the reactions; nt – non tested; Ct – cycle threshold value refers the number of cycles needed to replicate enough DNA/RNA for virus detection.

Table 5

Results of influence of ALBO nanosilver quantum dots filter on SARS-CoV-2 virus loads and viability without PMAxx

Label of samples	Control samples		Internal control[#]
	Labels	Ct values SARS-CoV-2	Ct values
Incubation 60 min (carried out comparatively and under the same conditions as the incubation of virus with test samples)	PC	15.75	36.75
	PC	15.41	35.33
	PC	15.47	36.47
	PC-P	28.33	31.76
	PC-P	8.49	31.41
	PC-P	28.33	31.59
	Water	No Ct (Ct > 50)	31.30
	Water	No Ct (Ct > 50)	31.39
	Water	No Ct (Ct > 50)	31.52
	NTC	No Ct (Ct > 50)	nt
	NTC	No Ct (Ct > 50)	nt
	NTC	No Ct (Ct > 50)	nt

For abbreviations, see Table 4.

For six test-performed copies, the average C_t value of PMAxx-treated samples by incubated SARS-CoV-2 viruses with an ALBO nanosilver Fs for 60 min was C_t 38.34, while the mean value of the virus tested with PMAxx was C_t 28.38. Based on the "viability PCR" method, the maximal difference between the control and test samples determined based on the "viability PCR" method was 10.67 C_t, and the smallest, 9.16 C_t values (average 38.34–26.38 = 9.96 C_t). Translated into the number of viral particles – detectable viable genome particles of SARS-CoV-2 virus, the difference between the tested ALBO nanosilver Fs material and untreated control samples (virus load used for experiment), i.e., the reduction in the number of viable viral particles (genomes), was from 2.75 $\log_{10}$ to 3.20 $\log_{10}$, with an average of 2.99 $\log_{10}$ of the number of detectable viable viral genomes.

Discussion

SEM and EDS confirmed the impregnation of Ag onto CFs. Inductively coupled plasma spectroscopy (ICP) proved the powerful bonding of Ag quantum dots with cotton fabric fibers, which is very important from the aspect of filter safety if used as a part of a face mask. Wettability measurements indicated a strong hydrophobicity of the filter surface. Knowing that the contact angle of 150° corresponds to the superhydrophobic properties of a given material [39–40], the obtained data show that the surface of ALBO nanosilver Fs has nearly hydrophobic properties. Therefore, it can be expected that instead of being absorbed on the surface of the filter cloth, a droplet containing viruses will roll like a ball on its surface. This is very important because it indicates a significantly reduced probability of deeper penetration of aerosol droplets into the volume of the ALBO nanosilver Fs. The color fastness test showed that the color fastness of the Ag-impregnated cotton fabric during rubbing in wet conditions was lower than in dry conditions in all washing cases. The increased affinity between hydroxyl and COOH groups of the cross-linking poly- COOH acid also influences stronger chemical bonding of Ag quantum dots with CFs [41]. These samples show significantly less morphological change of CFs during washing and, consequently, weakening of chemical bonds between the impregnated Ag quantum dots and the structure of CFs. Cross-linking inside of CFs is caused mainly by the reaction of the hydroxyl groups in cellulose and COOH group in poly- COOH acid and the formation of two or more ester bonds with cellulose macromolecules, resulting finally in cross-linking cotton fabric fiber structure. Since cellulose macromolecules consist of interconnected glucose rings and hydroxyl groups, which protrude from macromolecular chains, providing reactive cross-linking sites due to cross-linking reactions that occur in inaccessible regions with cellulose hydroxyl groups, this also results in better resistance from deformation [41, 42].

The antibacterial assay showed that nano-Ag impregnation of the fabric could not hold the growth of *S. aureus* in large numbers, but for amounts found in human surroundings, it showed an exemplary effect. With ambulance patient services total bacterial count of 468 ± 607 CFU/m^3 and housing air count of 158 CFU/m^3/day of *S. aureus*, we believe that we have achieved an exceptional reduction in the bacterial count for intended usage [32, 43]. We have experienced better results than the top coating of cotton fabric with nanoparticles, where less than 20% of starting inoculum was reduced after 4 hrs [44], while our high activity is comparable to findings of Emam et al. [45] as well as Deng et al. [46]. Lesser antibacterial effect in large inoculums may be due to the static method of incubation where bacteria have not had the opportunity to come in direct contact with material, as well as the short incubation period. The antibacterial activity of nano-Ag was found to be dependent on the shape and size of Ag particles [47].

The results of the "viability PCR" method, which detects the RNA genome of only viable (complete) viral particles, indicated that ALBO nanosilver Fs showed a significant antiviral effect on SARS-CoV-2 which was

reflected in a significant reduction in the number of detectable viral genome particles relative to the virus being tested. The results obtained from the real-time RT-PCR method indicate a significant antiviral effect of ALBO nanosilver Fs when testing the number of viable (complete infectious particles) SARS-CoV-2 virions. The reduction of viability of SARS-CoV-2 virus particles used for the experiment after the one-hour contact with ALBO nanosilver Fs was ≥ 2.99 $\log_{10}$, or about 1,000 times lower number of infectious virus particles, which implicated very high efficiency of ALBO nanosilver Fs in protection from SARS-CoV-2, which is the protection that far surpasses protection provided by any commercial mask available worldwide, including the FPP-2 and FPP-3 masks.

Conclusion

A new concept of manufacturing face masks for protection against bacteria and viruses, particularly SARS-CoV-2, was applied in this paper. This approach assumed the manufacturing of superhydrophobic, antibacterial, and anti-COVID active filters as the middle layer of a three-layer mask. These filters were made of dense cotton fabric impregnated with Ag quantum dots. *In vitro* investigations of these filters showed extremely high efficiency in destroying *S. aureus* bacteria and the SARS-CoV-2 virus. Additionally, the filters showed high safety and easy breathing, and, therefore, these masks can be a satisfactory solution during virus pandemics like the recent SARS-CoV-2 pandemic, particularly for the protection of medical staff working in highly virulent environments.

Acknowledgement

The research was funded by the Ministry of Science, Technological Development and Innovation of the Republic of Serbia (No. 451-03-47/2023-01/200017).

REFERENCES

1. *Rai M, Bonde S, Yadav A, Bhowmik A, Rathod S, Ingle P,* et al. Nanotechnology as a Shield against COVID-19: Current Advancement and Limitations. Viruses 2021; 13(7): 1224.
2. *Jokanović V, Živković M, Zdravković N.* A new approach to extraordinary efficient protection against COVID 19 based on nanotechnology. Stomatol Glas Srb 2020; 67(2): 100–9.
3. *MacIntyre CR, Seale H, Dung TC, Hien NT, Nga PT, Chughtai AA,* et al. A cluster randomised trial of cloth masks compared with medical masks in healthcare workers. BMJ Open 2015; 5(4): e006577.
4. *Leung NHL, Chu DKW, Shiu EYC, Chan KH, McDevitt JJ, Hau BJP,* et al. Respiratory virus shedding in exhaled breath and efficacy of face masks. Nat Med 2020; 26(5): 676–80. Erratum in: Nat Med 2020; 26(6): 981.
5. *Shi J, Zou Y, Wang JX, Zeng XF, Chu GW, Sun BC,* et al. Investigation on Designing Meltblown Fibers for the Filtering Layer of a Mask by Cross-Scale Simulations. Ind Eng Chem Res 2021; 60(4): 1962–71.
6. *MacIntyre CR, Chughtai AA.* A rapid systematic review of the efficacy of face masks and respirators against coronaviruses and other respiratory transmissible viruses for the community, healthcare workers and sick patients. Int J Nurs Stud 2020; 108: 103629.
7. *He J, Zhao H, Li X, Su D, Zhang F, Ji H,* et al. Superelastic and superhydrophobic bacterial cellulose/silica aerogels with hierarchical cellular structure for oil absorption and recovery. J Hazard Mater 2018; 346: 199–207.
8. *Xuao FX, Pagliaro M, Xu YJ, Liu B.* Layer-by-layer assembly of versatile nanoarchitectures with diverse dimensionality: a new perspective for rational construction of multilayer assemblies. Chem Soc Rev 2016; 45(11): 3088–121.
9. *Emam HE, Mowafi S, Mashaly HM, Rehan M.* Production of antibacterial colored viscose fibers using in situ prepared spherical Ag nanoparticles. Carbohydr Polym 2014; 110: 148–55.
10. *Chakraborty D, Kumar S, Chandrasekaran N, Mukherjee A.* Viral Diagnostics and Preventive Techniques in the Era of COVID-19: Role of Nanoparticles. Front Nanotechnol 2020; 2: 588795.
11. *Wei DW, Wei H, Gauthier AC, Song J, Jin Y, Xiao H.* Superhydrophobic modification of cellulose and cotton textiles: Methodologies and applications. J Biores Bioprod 2020; 5(1): 1–15.
12. *Wyszogrodzka G, Marszałek B, Gil B, Dorożyński P.* Metal-organic frameworks: mechanisms of antibacterial action and potential applications. Drug Discov Today 2016; 21(6): 1009–18.
13. *Black JG.* Microbiology: principles and applications. 3rd ed. Upper Saddle River, NJ: Prentice Hall; 1996. 880 p.
14. *Rodríguez RA, Pepper IL, Gerba CP.* Application of PCR-based methods to assess the infectivity of enteric viruses in environmental samples. Appl Environ Microbiol 2009; 75(2): 297–307.
15. *Huntley CJ, Crews KD, Curry ML.* Chemical Functionalization and Characterization of Cellulose Extracted from Wheat Straw Using Acid Hydrolysis Methodologies. Int J Polym Sci 2015; (11): 1–9.
16. *Smiechowicz E, Niekraszewicz B, Kulpinski P.* Optimisation of AgNP Synthesis in the Production and Modification of Antibacterial Cellulose Fibres. Materials (Basel) 2021; 14(15): 4126.
17. *Fuster N, Pintó RM, Fuentes C, Beguiristain N, Bosch A, Guix S.* Propidium monoazide RTqPCR assays for the assessment of hepatitis A inactivation and for a better estimation of the health risk of contaminated waters. Water Res 2016; 101: 226–32.
18. *Shah SR, Kane SR, Elsheikh M, Alfaro TM.* Development of a rapid viability RT-PCR (RV-RT-PCR) method to detect infectious SARS-CoV-2 from swabs. J Virol Methods 2021; 297: 114251.
19. *Wurtzer S, Waldman P, Ferrier-Rembert A, Frenois-Veyrat G, Mouchel JM, Boni M,* et al. Several forms of SARS-CoV-2 RNA can be detected in wastewaters: Implication for wastewater-based epidemiology and risk assessment. Water Res 2021; 198: 117183.
20. *Polo D, Lois M, Fernández-Núñez MT, Romalde JL.* Detection of SARS-CoV-2 RNA in bivalve mollusks and marine sediments. Sci Total Environ 2021; 786: 147534.
21. *Cangelosi GA, Meschke JS.* Dead or alive: molecular assessment of microbial viability. Appl Environ Microbiol 2014; 80(19): 5884–91.
22. *Corman VM, Landt O, Kaiser M, Molenkamp R, Meijer A, Chu DK,* et al. Detection of 2019 novel coronavirus (2019-nCoV) by real-time RT-PCR. Euro Surveill 2020; 25(3): 2000045. Erratum in: Euro Surveill 2020; 25(14): 20200409c. Erratum

in: Euro Surveill 2020; 25(30): 2007303. Erratum in: Euro Surveill 2021; 26(5): 210204e.
23. *Tang YW, Stratton CW*. Staphylococcus aureus: An old pathogen with new weapons. Clin Lab Med 2010; 30(1): 179–208.
24. *Miller LG, Kaplan SL*. Staphylococcus aureus*:* A community pathogen. Infect Dis Clin North Am 2009; 23(1): 35–52.
25. *Payne SC, Benninger MS*. Staphylococcus aureus is a major pathogen in acute bacterial rhinosinusitis: a meta-analysis. Clin Infect Dis 2007; 45(10): e121–7.
26. *Kaplan SL, Hulten KG, Gonzalez BE, Hammerman WA, Lamberth L, Versalovic J,* et al. Three-year surveillance of community-acquired Staphylococcus aureus infections in children. Clin Infect Dis 2005; 40(12): 1785–91.
27. *Savić Radovanović R, Zdravković N, Velebit B*. Occurrence and Characterization of Enterotoxigenic Staphylococci Isolated from Soft Cheeses in Serbia. Acta Vet 2020; 70(2): 238–54.
28. *Goggin R, Jardeleza C, Wormald PJ, Vreugde S*. Colloidal silver: a novel treatment for Staphylococcus aureus biofilms? Int Forum Allergy Rhinol 2014; 4(3): 171–5.
29. *Grigor'eva A, Saranina I, Tikunova N, Safonov A, Timoshenko N, Rebrov A,* et al. Fine mechanisms of the interaction of silver nanoparticles with the cells of Salmonella typhimurium and Staphylococcus aureus. Biometals 2013; 26(3): 479–88.
30. *Deng X, Nikiforov AY, Coenye T, Cools P, Aziz G, Morent R,* et al. Antimicrobial nano-silver non-woven polyethylene terephthalate fabric via an atmospheric pressure plasma deposition process. Sci Rep 2015; 5: 10138.
31. *Jia M, Chen Z, Guo Y, Chen X, Zhao X*. Efficacy of silk fibroin–nano silver against Staphylococcus aureus biofilms in a rabbit model of sinusitis. Int J Nanomedicine 2017; 12: 2933–9.
32. *Peroja KAG, Tuberon NAL, Garcia KA*. A review of metal nanoparticles incorporated in polymer matrices for water disinfection. Global Sci J 2019; 7(2): 264–311.
33. *Mackay IM, Arden KE, Nitsche A*. Real-time PCR in virology. Nucleic Acids Res 2002; 30(6): 1292–305.
34. *Kageyama T, Kojima S, Shinohara M, Uchida K, Fukushi S, Hoshino FB,* et al. Broadly reactive and highly sensitive assay for Norwalk-like viruses based on real-time quantitative reverse transcription-PCR. J Clin Microbiol 2013; 41(4): 1548–57.
35. *Leifels M, Cheng D, Sozzi E, Shoults DC, Wuertz S, Mongkolsuk S,* et al. Capsid integrity quantitative PCR to determine virus infectivity in environmental and food applications - A systematic review. Water Res X 2020; 11: 100080.
36. *Blanco A, Guix S, Fuster N, Fuentes C, Bartolomé R, Cornejo T,* et al. Norovirus in Bottled Water Associated with Gastroenteritis Outbreak, Spain, 2016. Emerg Infect Dis 2017; 23(9): 1531–4. Erratum in: Emerg Infect Dis 2017; 23(11): 1937.
37. *Randazzo W, Khezri M, Ollivier J, Le Guyader FS, Rodríguez-Díaz J, Aznar R*, et al. Optimization of PMAxx pretreatment to distinguish between human norovirus with intact and altered capsids in shellfish and sewage samples. Int J Food Microbiol 2008; 266: 1–7.
38. *Terio V, Lorusso V, Mottola A, Buonavoglia C, Tantillo G, Bonerba E,* et al. Norovirus Detection in Ready-To-Eat Salads by Propidium Monoazide Real Time RT-PCR Assay. Appl Sci 2020; 10(15): 5176.
39. *Čolović B, Kisić D, Jokanović B, Rakočević Z, Nasov I, Trajkovska Petkovska A*, et al. Wetting properties of titanium oxides, oxynitrides and nitrides obtained by DC and pulsed magnetron sputtering and cathodic arc evaporation. Mater Sci Pol 2019; 37(2): 173–81.
40. *Parvate S, Dixit P, Chattopadhyay S*. Superhydrophobic Surfaces: Insights from Theory and Experiment. J Phy Chem B 2020; 124(8): 1323–60.
41. *Montazer M, Alimohammadi F, Shamei A, Rahimi MK*. Durable antibacterial and cross-linking cotton with colloidal silver nanoparticles and butane tetracarboxyl ic acid without yellowing. Colloids Surf B Biointerfaces 2012; 89: 196–202.
42. *Hameed S, Hussain MA, Masood R, Haseeb MT*. Cross-linking of cotton fabric using maleic anhydride and sodium hypophosphite. Cellul Chem Technol 2016; 50(2): 321–8.
43. *Kumar TVC, Prasad TNVK, Adilaxmamma K, Alpharaj M, Muralidhar Y, Prasad PE*. Novel synthesis of nanosilver particles using plant active principle aloin and evaluation of their cytotoxic effect against Staphylococcus aureus. Asian Pac J Trop Dis 2014; 4(Suppl 1): S92–6.
44. *Thanh NVK, Phong NTP*. Investigation of antibacterial activity of cotton fabric incorporating nano silver colloid. J Phys Conf Ser 2009; 187(1): 012072.
45. *Emam HE, Manian AP, Široká B, Duelli H, Redl B, Pipal A,* et al. Treatments to impart antimicrobial activity to clothing and household cellulosic-textiles - why "Nano"-silver? J Clean Prod 2013; 39(4): 17–23.
46. *Deng X, Nikiforov A, Vujosevic D, Vuksanovic V, Mugoša B, Cvelbar U,* et al. Antibacterial activity of nano-silver non-woven fabric prepared by atmospheric pressure plasma deposition. Mat Lett 2015; 149: 95–9.
47. *Sadeghi B, Garmaroudi FS, Hashemi M, Nezhad HR, Nasrollahi A, Ardalan S,* et al. Comparison of the anti-bacterial activity on the nanosilver shapes: Nanoparticles, nanorods and nanoplates. Adv Powder Technol 2012; 23(1): 22–6.

Received on September 22, 2023
Accepted on February 20, 2024
Online First April 2024